Scripta Materialia 144 (2018) 27–30

Contents lists available at ScienceDirect

Scripta Materialia

journal homepage: www.elsevier.com/locate/scriptamat

Regular Article

Enhanced red emission from Fe/Si co-doped ZnO nano-particles

Gaurav Bajpai [a], Tulika Srivastava [a], Faizan Husian [a], Sunil Kumar [a], Sajal Biring [c], Somaditya Sen [a,b,*]

[a] Metallurgy Engineering and Material Science, Indian Institute of Technology Indore, India
[b] Department of Physics, Indian Institute of Technology Indore, India
[c] Electronic Engg., Ming Chi University of Technology, New Taipei City, Taiwan

ARTICLE INFO

Article history:
Received 9 August 2017
Accepted 25 September 2017
Available online xxxx

Keywords:
ZnO
Photoluminescence
Bandgap
Oxygen interstitials

ABSTRACT

Structural, optical, and photoluminescence properties of $Zn_{0.95}Si_{0.05-x}Fe_xO$ ($0 \le x \le 0.05$) nano-crystallites prepared by sol-gel process has been investigated thoroughly revealing enhanced red emission in co-doped samples originating from oxygen interstitials. Greater ionic charge and smaller size of the substituent ions helps generate more interstitials forming defect states within the bandgap. The correlation between oxygen interstitials, i.e. defect states corresponding to the doping concentrations of Si and Fe ions and the enhanced red emissions from the samples has been established unequivocally following a quantitative approach by analyzing the photoluminescence spectra contributed from the individual defect levels.

Zinc oxide (ZnO), a wide-bandgap (3.37 eV) group II–VI semiconductor with high electron mobility, shows strong room-temperature luminescence [1] and good optical transparency at UV–visible region. ZnO photoluminescence is typically subdivided into two regions. A near band edge emission (NBE) is observed in violet-UV region. The deep level emission (DLE) is a broad spectrum originated from the defects in the bandgap away from the band edges. In spite of a controversial origin [2–7] of defect emission, it is generally accepted that green emission is associated with oxygen deficiency while orange-red emission, being rarely found, is associated with excess of oxygen [8–11].

Doping affects luminescence of ZnO, e.g. red emission in Co doped ZnO [12], yellow-orange-red emission in Mn doped ZnO [13], blue emission in Cu doped ZnO [14], orange emission in Si doped ZnO [15]etc. Fe/Si co-substituted ZnO system is a new way of looking into luminescence to understand the nature of the bonding between dopant ions and oxygen. This has not been studied thoroughly. The 4+ and 3+ oxidation states of Si^{4+} and Fe^{3+} respectively as compared to the 2+ state of Zn^{2+} should allow the lattice to hold more oxygen, thereby reduce oxygen defects and create O interstitials. In this report we will analyze the defect states and justify bandgap modifications of $Zn_{0.95}Si_{0.05-x}Fe_xO$ nano-particles.

$Zn_{0.95}Si_{0.05-x}Fe_xO$ nanoparticles with x = 0, 0.02, 0.03 and 0.05 respectively have been synthesized by standard Pechini sol-gel process followed by solid state sintering. Dissolving ZnO powder in HNO_3 (Alfa Aesar, purity 99.9%) and adding appropriate amount of $Fe(NO_3)_3 9H_2O$ (Ferric Nitrate Nonahydrate), $(C_2H_5O)_4Si$) (Tetraethyl orthosilicate), a homogeneous solution was prepared by prolonged stirring. Citric acid and glycerol were used as gelling agent. Burnt gels were decarbonized and denitrified at 450 °C for 6 h followed by annealing at 600 °C for 2 h in air flow.

The surface morphology investigated by Field Emission Scanning Electron microscopy (Carl Zeiss FESEMSupra-55) [Fig. 1(a) inset] reveals uniform and homogeneous spherical nano-particle of size ~50 nm for all doped and undoped samples.

X-ray diffraction confirmed dominant hexagonal phase of the materials with two negligible zinc blend peaks (even in pure ZnO) but no other unwanted phase [Fig. 1(a)]. The lattice parameters, average crystalline size, and strain of $Zn_{0.95}Si_{0.05-x}Fe_xO$ nano-particles [Fig. 1(b)] were estimated from XRD data using GSAS software. Crystallite size was estimated using Debye Scherrer equation, $D = 18{,}000(K\lambda)/(\pi L_X)$; where, $K = 1$ is a constant, while strain was calculated using $S = (\pi L_y)/18{,}000$. Particle size, lattice parameters, 'a', 'c' and 'c/a' ratio decreased, while strain increased with substitution [Fig. 1(b)]. Note that although Si^{4+}(IV)[~0.4 Å] is much smaller than Zn^{2+}(IV)(~0.74 Å), the lattice parameters shrink nominally for purely Si substitution. In fact lattice shrinks at a faster rate with the substitution of Si by Fe^{3+}(IV)(~0.63 Å) which is much larger than Si. Note that the charge of Fe^{3+} is also lesser than Si^{4+}.

Optical transmittance data was obtained using Agilent UV–vis spectrometer (model Carry 60) [Fig. 2(a)]. From the extrapolated slopes of the data it was observed that the band gap (E_g) of pure ZnO was ~3.24 eV. In a previous study, E_g was reported as ~3.13 eV. This difference was obtained from annealing the samples in slightly different techniques. In the previous report with pure Si doping (substitution ≤ 3%) it has been presented that E_g showed a trend of a nominal increase while Urbach energy, ΔU, i.e. lattice strain, decreased [16–21]. The Urbach energy, ΔU, was estimated from the relation, $\alpha = \alpha_o \exp(h\nu/\Delta U)$ near the tailing edges of the absorption spectra [Fig. 2(c)]. Better crystalline,

---

[*] Corresponding author at: Metallurgy Engineering and Material Science, Indian Institute of Technology Indore, India.

E-mail address: sens@iiti.ac.in (S. Sen).

https://doi.org/10.1016/j.scriptamat.2017.09.041
1359-6462/

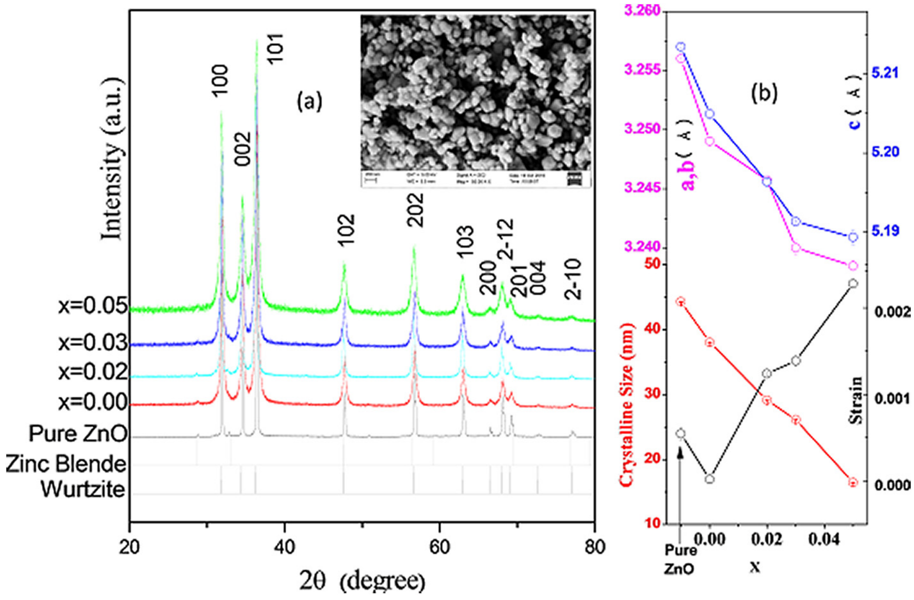

Fig. 1. (a) XRD pattern of $Zn_{0.95}Si_{0.05-x}Fe_xO$ ($0 \leq x \leq 0.05$), 1(a) inset FESEM image, (b) crystalline size, strain and lattice parameter with doping.

undistorted lattice (due to more oxygen retention capability of greater charged Si^{4+}) resulted in reduction of lattice strain. As a result bandgap increased marginally due to lessening of defect states near the band edge.

In this study we observe a similar scenario; the starting material, $x = 0$, is ~5% Si-substituted ZnO, in which, E_g increased to 3.26 eV as compared to 3.24 eV in pure ZnO. Urbach energy is higher in pure ZnO ($\Delta U = 37$ meV) than the purely Si doped sample (i.e. $x = 0$) ($\Delta U = 36.6$ meV). However, as we gradually replace Si with Fe the bandgap decreases from 3.26 eV in $x = 0$ to 3.18 eV in $x = 0.05$ (Fig. 2b). Band edge tailing, i.e. lattice strain starts with Fe incorporation. [Fig. 2(b)]. Tailing of band edges of both conduction band as well as valence band narrows the band gap. This results in decreasing bandgap and increasing Urbach energy [Fig. 2(b)]. With Fe incorporation it increases from 36.6 meV for $x = 0.00$ to 245 meV for $x = 0.05$.

From the above trend, an anomaly is observed. The effect of introducing Fe^{3+} is exactly opposite to that of Si^{4+} although the crystal radius of Si is smaller than Fe. One should expect greater strain in case of Si substitution than Fe substitution, contrary to what is observed. To be noted is that the energy levels created by Si are located outside the bandgap of ZnO [22]. Due to the small size of Si^{4+}, the electrons in Si do not involve in strong overlapping with the electrons in O. As a result the bonding between Si and O does not strain the lattice. However, hybridization between localized Fe d and O s/p electrons creates levels

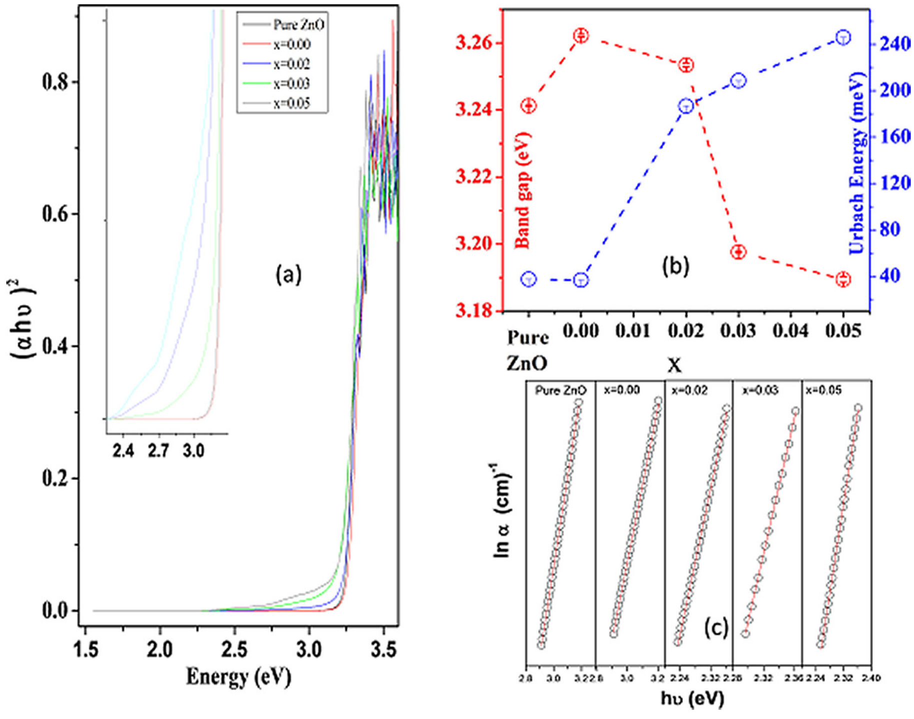

Fig. 2. (a) Optical transmittance of $Zn_{0.95}Si_{0.05-x}Fe_xO$ ($0 \leq x \leq 0.05$), (b) Bandgap and Urbach energy versus x, (c) linear fit of Urbach tail.